NASA CONTRACTOR REPORT

NASA-CR-3

NASA CR-339

SINGLE PARAMETER TESTING APPLICATION

by E. L. Berger and J. C. Jackson

Prepared under Contract No. NASA-8-11715, Part III, *by*
GENERAL ELECTRIC COMPANY
Daytona Beach, Fla,
for George C. Marshall Space Flight Center

NATIONAL AERONAUTICS AND SPACE ADMINISTRATION - WASHINGTON, D. C. - DECEMBER 1965

SINGLE PARAMETER TESTING APPLICATION

By E. L. Berger and J. C. Jackson

Prepared under Contract No. NASA-8-11715, Part III, by
GENERAL ELECTRIC COMPANY
Daytona Beach, Fla.

for George C. Marshall Space Flight Center

NATIONAL AERONAUTICS AND SPACE ADMINISTRATION

For sale by the Clearinghouse for Federal Scientific and Technical Information
Springfield, Virginia 22151 – Price $2.00

TABLE OF CONTENTS

LIST OF ILLUSTRATIONS

SECTION 1

INTRODUCTION

GENERAL

The single parameter testing program in Phase C is specifically designed to select an actual subsystem for analysis, with the guidance and approval of the NASA technical representative. The transfer function will be derived and the techniques developed in Phases A and B will be applied to the subsystem.

The purpose of this task is to apply single parameter testing to a practical system. To meet this purpose, several factors will have to be established:

a. First, the testing of a practical system involves the determination of the most important parameters of the system. Parameters which are highly reliable and relatively insensitive are of little concern. The only exception that may be made is to assert that the system is working. Once it has been established that the system is functioning, it can be asserted with confidence that the insensitive and highly reliable parameters are functioning properly. Therefore, the important parameters must be determined.

b. Second, the method of measuring a highly complex system to extract the important parameters must be considered. The methods that may be available can be generalized to make assumptions concerning the testing of the system.

   Basically, these assumptions will consist of:

   (1) Simplifying the system.
   (2) Reducing the number of parameters to be tested.
   (3) Linearizing the system.

   These assumptions may be valid and result in simplified procedures for measurements. On the other hand, they may decrease the accuracy and effectiveness of single parameter testing.

c. Finally, practical problems may be encountered in the measurements which have not been included in the system model. While these practical problems are relatively unknown for a particular system, their existence is to be expected. These problems should not be considered as a limitation of single parameter testing, but rather one of equipment limitations. It is entirely possible that the practical problems can be eliminated by proper design of equipment to apply the single parameter testing procedure.

The factors previously mentioned are essential in order to fully understand the analysis discussed in this report. In each of the following sections, certain assumptions were made. In Section 2 the results of testing an X-Y plotter are presented. Section 3 contains the planned approach to testing a positioning servo system. The assumptions made on the testing of each piece of equipment are different. The assumptions made on the testing of the positioning system are based on the results obtained from testing the X-Y plotter.

SECOND ORDER SERVO-LOOP TESTING

The technical approach of single parameter testing with growing exponential signals was applied to the servo-loop controlling position on an X-Y plotter. The primary purpose of the test was to establish the test procedure for a physical system and gain insight into practical limitations. The testing was necessary for a theoretical examination of higher order, or of more complex systems because evaluation of various poles ignored in the model development could show their practical effect.

In general the results of the tests on the X-Y plotter are weaker than initially expected since no specific quantitative results can be stated. However, qualitative results pertinent to the general testing philosophy and the observations made during the tests showed an improved testing procedure for more complex systems.

The main conclusions obtained from the experimental work on the X-Y plotter arm position control loop are:

a. The practical sensitivity or measurability of the growing exponential technique to variations in parameter values depends strongly on how close the input probing signal is matched to the partial derivative of the system function. This signal match requires accurate coefficient values in the transfer function of the nominal system. As a practical consideration, some systems may require an extensive evaluation of the system operation to obtain these transfer function coefficients.

b. The instrumentation for implementing the entire method must be highly compatible with input/output impedance relations and signal levels on the actual transfer function under evaluation. In some instances, the transfer characteristic to and from the measuring instrumentation to the actual system may require accurate transfer function evaluation.

c. Based on the testing problems encountered on the servo loop, investigation into the complex position control loop is substantiated with details to more fully describe the operating transfer function.

The data shown in Figure 1-1 includes the input probing signal matched to $H_1(S)$ and the difference in the response of each of the two X-Y plotter servo loops. (For a nominal system, a second X-Y plotter servo loop was used.)

Figure 1-2 illustrates the response from each of the servo loops separately. Figure 1-3 shows a gain change in each servo loop observed at the estimator output terminal. Figures 1-4 and 1-5 indicate the respective changes in each recorder (+ 100 percent, 0, -50 percent). Finally, Figure 1-6 shows two separate levels of limiting the servo travel.

The second order transfer function for the servo loop investigated is:

$$H_1(S) = \frac{K}{S^2 + 15.085 + 184.4} \tag{1-1}$$

The total transfer function, obtained by a detailed analysis and measured data is:

$$H_T(S) = \frac{K(S + 275)}{(S^2 + 15.08S + 184.4)(S + 81.5)(S + 279)} \tag{1-2}$$

In review, it can be stated that the following reasons accounted for the difficulties in obtaining quantitative results:

a. The approximation of the transfer function in forming the matching input signal.
b. Nonlinear effects introduced by the chopper and motor modulation demodulation characteristic.
c. Signal levels from the servo loop required large gains to be compatible with the computer signal levels.

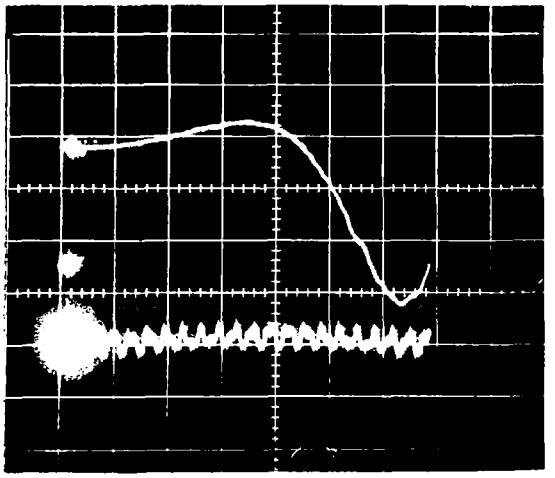

Figure 1-1. Input Probing Signal - System A Minus System B Response

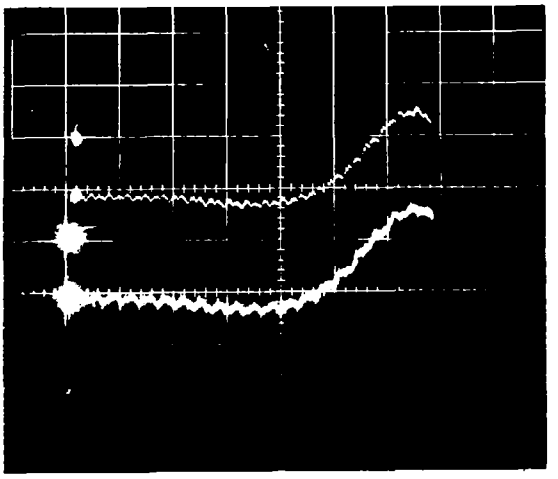

Figure 1-2. Servo-Loop Response
a. System A Response
b. System B Response

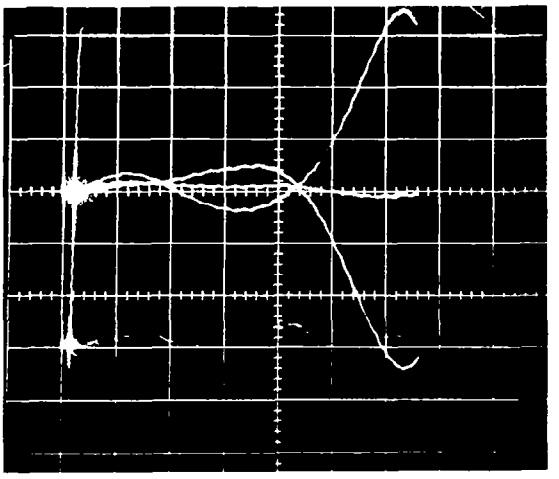

Figure 1-3. Gain Change at Estimator Output

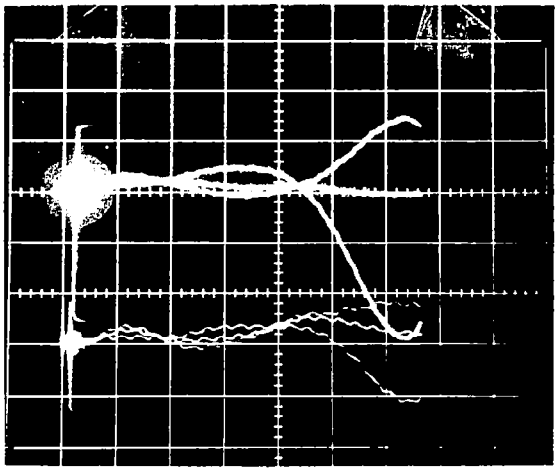

Figure 1-4. Gain Change at Estimator Output - System A

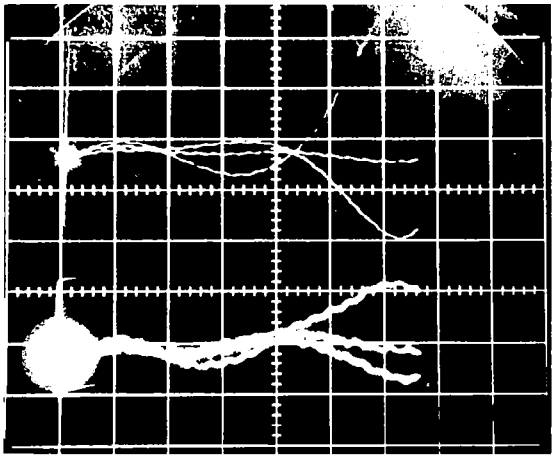

Figure 1-5. Gain Change at Estimator Output - System B

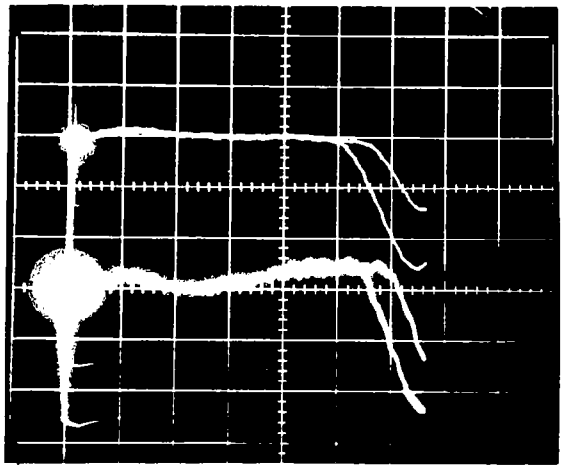

Figure 1-6. Position Limiting

SECTION 2

ANALYSIS AND DISCUSSION

The first part of this discussion is devoted to a basic analysis of the servo-loop controlling arm position on an X-Y plotter. The second part is devoted to the test requirements and experimental results.

The basic servo loop includes an input attenuator, a chopper network, a servo amplifier, a two-phase a-c motor, and a compensation network that feeds back voltage proportional to position. A block diagram is shown in Figure 2-1.

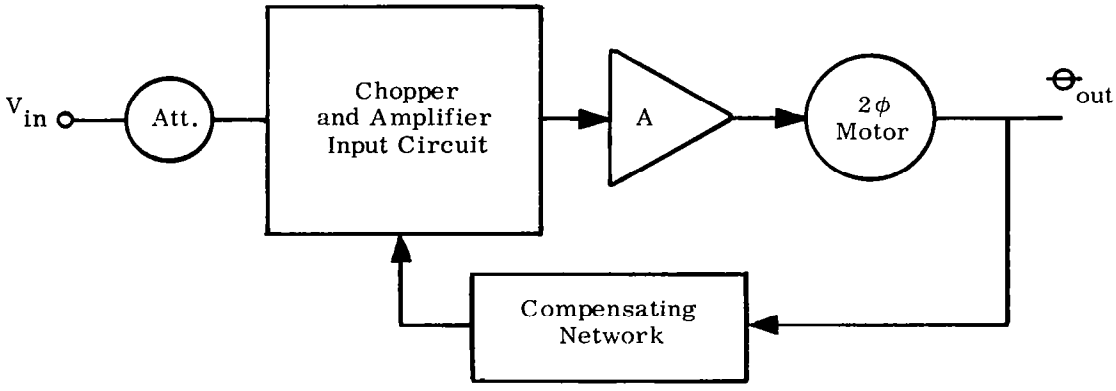

Figure 2-1. Basic Servo Loop

The chopper and two-phase a-c motor form a modulation demodulation combination so that the amplifier gain characteristics are of the a-c type. References 1 and 2 indicate that a reasonable model for this combination contains a d-c amplifier, a low-pass filter, and a d-c motor. Various assumptions used in picking this model are governed by techniques and requirements for control system design and are discussed in the references. However, the main concern in this report includes an evaluation of parameters in the model and consequently assumption validity must be considered.

The major assumptions include perfect modulation in the chopper and demodulation in the motor, flat amplifier response over the range of validity of the model, and no dependency of motor characteristics on the input signal. For the servo loop on the X-Y

plotter arm position, all three assumptions are questionable. The output from the chopper has a strong third harmonic, the amplifier is not exceptionally flat, and the motor characteristic is apparently dependent upon the amplifier input; however, the over-all system response appears to follow the linear assumption predictions in magnitude and phase response.

A block diagram of the model used for the servo loop is shown in Figure 2-2.

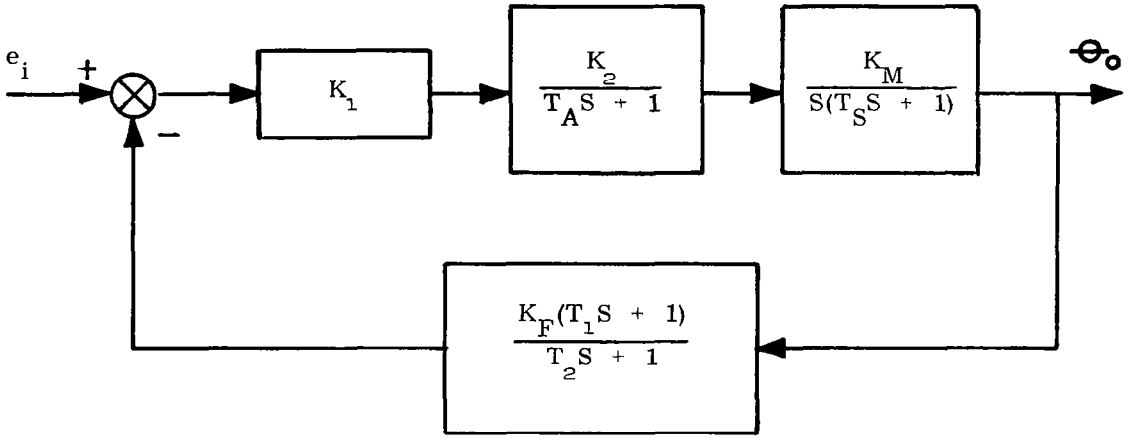

Figure 2-2. Simplified Model of Arm Position Control Loop

NOTE

Compensator Constants

The signal input to the compensating network is a voltage supplied by a d-c bridge network. The bridge network output voltage is proportional to the arm position plus a small d-c voltage. A model for the feedback compensation is shown in Figure 2-3.

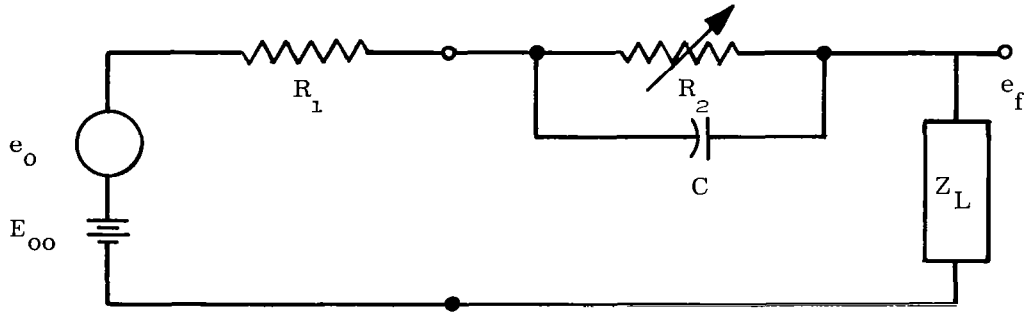

Figure 2-3. Equivalent Compensation Network

Based on this network the output voltage is:

$$e_f = \frac{Z_L (1 + SCR_2) (e_o + E_{oo})}{SCR_2 (R_1 + Z_L) + Z_L + (R_1 + R_2)} \qquad (2\text{-}1)$$

where

e_o - Is the position indicating component of voltage of the bridge network.

Z_L - Is the load impedance at the chopper input.

e_f - Is the feedback voltage at the chopper input.

The numerator time constant is:

$$T_1 = R_2C$$

From the form of Equation 2-1 the denominator equivalent time constant is:

$$T_2 = \frac{CR_1 (R_1 + Z_L)}{R_2 + (R_1 + Z_L)} \qquad (2\text{-}2)$$

or

$$T_2 = T_1 \left(\frac{R_1 + Z_L}{R_2 + R_1 + Z_L} \right) \qquad (2\text{-}3)$$

Note, this time constant is valid for Z_L only as a real number or pure resistance. Any reactance in the load modifies the interpretation of T_2 as a time constant; however, the relative magnitude of T_1 compared to T_2 is fixed. Clearly Equation 2-3 shows that T_2 is always less than T_1.

Next the two time-constants associated with the motor and equivalent low-pass filter were estimated after some trial and error calculations, and consideration of variable resistor limits and stability. The final open loop function is:

$$G(S)\,H(S) = K\left[\frac{1}{S(S + 12.6)(S + 94)}\right]\left[\frac{(S + 42)}{(S + 275)}\right] \qquad (2\text{-}4)$$

A root locus plot of this open loop transfer function is shown in Figure 2-4.

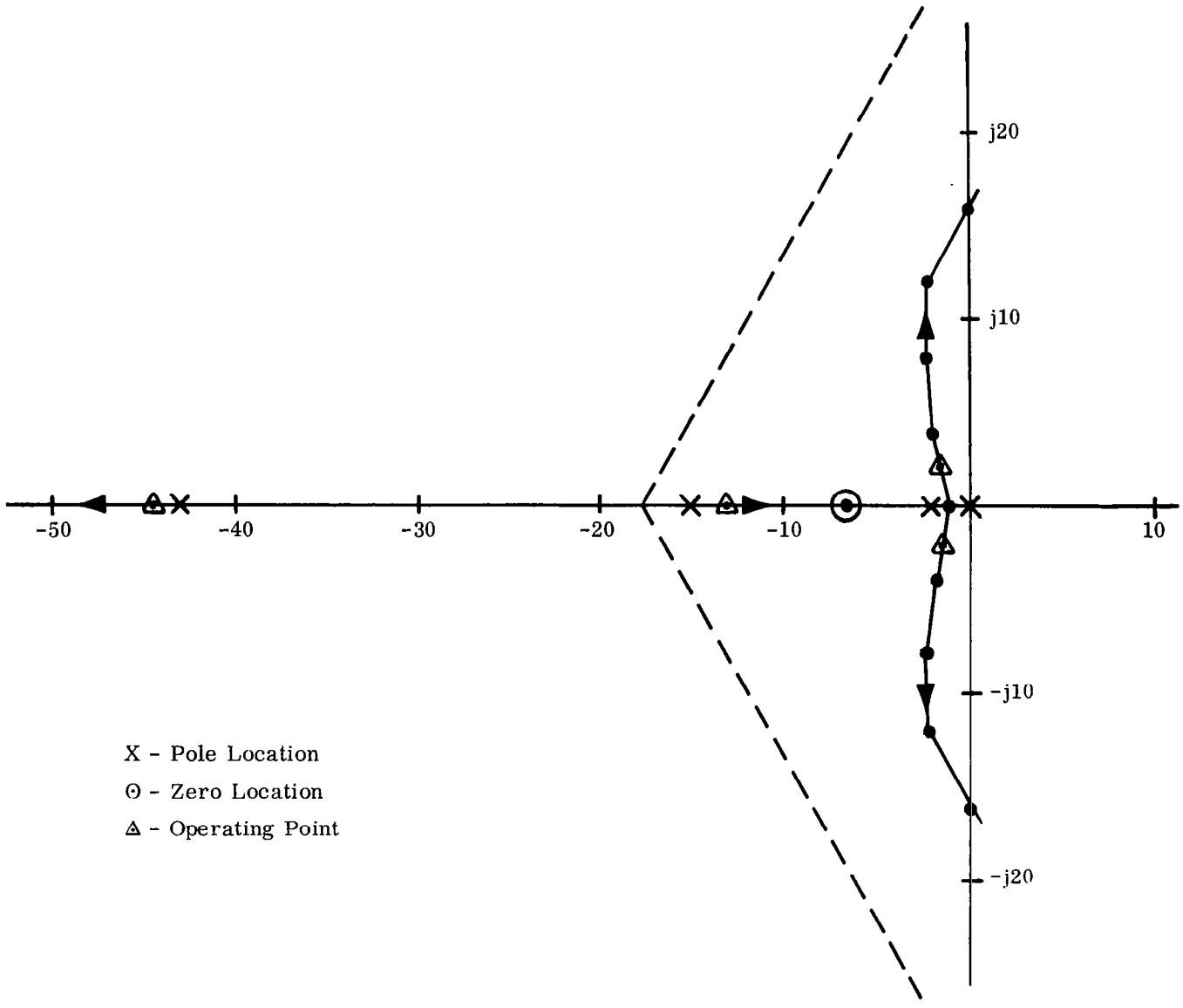

Figure 2-4. Root Locus for the Arm Position Control Loop on the X-Y Plotter

The closed loop operating transfer function is:

$$\frac{\Theta_o(S)}{V_{in}(S)} = \frac{K(S + 275)}{\left[(S + 7.54)^2 + (11.3)^2\right](S + 81.5)(S + 279)} \tag{2-5}$$

As a first approximation this transfer function is a simple second-order system, that is,

$$\frac{\Theta_o(S)}{V_{in}(S)} \approx \frac{K_1}{(S + 7.54)^2 + (11.3)^2} \tag{2-6}$$

Consideration of a compensating network to account for a pole at S = 81.5 yields:

$$G_{com} = \frac{-K_1}{(S + 7.54)^2 + (11.3)^2}\left(\frac{S + 80.5}{S + 81.5}\right) \tag{2-7}$$

NOTE

This compensation transfer function is obtained by methods presented in the Phase B report.

Considering the relative position of the pole and zero in the compensating transfer function, computer simulation of the calculated pole and zero, and approximation to the actual effect of the compensator from the root locus plot, the pole at S = 81.5 was dropped. Hence, the control loop transfer function in Equation 2-6 is assumed to approximate the actual response obtained from the X-Y plotter.

Expanding Equation 2-6 yields:

$$\frac{\Theta_o(S)}{V_{in}(S)} = \frac{K_1}{S^2 + 15.08\,S + 184.4} \tag{2-8}$$

The general form of Equation 2-8 is:

$$H(S) = \frac{\Theta_o(S)}{V_{in}(S)} = \frac{K_1}{S^2 + d_1 s + d_o} \tag{2-9}$$

The partial derivative systems are:

$$\frac{\partial H(S)}{\partial d_1} = \frac{-K_1 S}{(S^2 + d_1 S + d_o)} \tag{2-10}$$

$$\frac{\partial H(S)}{\partial d_o} = \frac{-K_1}{(S^2 + d_1 S + d_o)^2} \tag{2-11}$$

At this point the probing signals from page 42 of the Phase A report can be used to describe the partial derivative systems and specify coefficients in the computer implementation of a signal generator and filter pair.

Implementation of the single parameter testing procedure requires the following:

a. Coefficients for generating the input probing signal on the computer.
b. Coefficients for the simulated filters that match components of the output signal.
c. Estimator coefficients.
d. Coefficients for the transfer function simulation.

As a first step, consider the Katz functions from the Phase A report for a second-order system.

$$\Phi_1(+S) = \sqrt{2\alpha}\ \frac{(S + \omega_o)}{(S + \alpha)^2 + \beta^2} \tag{2-12}$$

$$\Phi(+S) = \sqrt{2\alpha}\ \frac{(S - \omega_o)\left[(S - \alpha)^2 + \beta^2\right]}{\left[(S + \alpha)^2 + \beta^2\right]^2} \tag{2-13}$$

The first function Φ_1, is relatively easy to invert into a time function, so consideration is given to the second function. The objective is to obtain the time response of $\Phi_2(+S)$, shift the resulting function back five time-constants, and reverse the time parameter. The resulting function is a rising exponential function that starts at a small value, namely minus five time-constants, and grows to unity at time zero.

This is accomplished by multiplying out the numerator terms to the form

$$\Phi_2(S) = \frac{S^3 + a_2 S^2 + a_1 S + a_0}{\left[(S + \alpha)^2 + \beta^2\right]^2} \tag{2-14}$$

Next the α term is removed or shifted by letting

$$S_1 = S - \alpha \tag{2-15}$$

then,

$$\Phi_2(S_1) = \frac{S_1^3 + a_{21} S_1^2 + a_{11} S_1 + a_{01}}{\left(S^2 + \beta^2\right)^2} \tag{2-16}$$

where the modified numerator coefficients are:

$$a_{21} = a_2 - 3\alpha \tag{2-17}$$

$$a_{11} = a_1 + 3\alpha^2 - 2\alpha a_2 \tag{2-18}$$

$$a_{01} = a_0 - a_1\alpha + \alpha^2 a_2 - \alpha^3 \tag{2-19}$$

NOTE

Second subscript (1) indicates shifted S, that is, $S_1 = S - \alpha$.

Next, by separating terms

$$\Phi_{21}(S_1) = \frac{a_{21} S_1^2 + a_{01}}{\left(S_1^2 + \beta^2\right)^2} + \frac{S_1(S_1^2 + a_{11})}{\left(S_1^2 + \beta^2\right)^2} \tag{2-20}$$

Then, rearranging the first term

$$\frac{a_{21} S_1^2 + a_{01}}{\left(S_1^2 + \beta^2\right)^2} = \frac{a_{21}(S_1^2 - \beta) + (a_{01} + \beta^2 a_{21})}{\left(S_1^2 + \beta^2\right)^2} \tag{2-21}$$

and rearranging the second term

$$\frac{S_1(S_1^2 + a_{11})}{\left(S_1^2 + \beta^2\right)^2} = \frac{S_1(S_1^2 + \beta^2) + S_1(a_{11} - \beta^2)}{\left(S_1^2 + \beta^2\right)^2} \tag{2-22}$$

The resulting expressions are ready for inversion by the use of tables since they appear in standard form. The resulting time function is:

$$f_{21}(t) = a_{21} t \cos \beta t + \frac{a_{01} + \beta^2 a_{21}}{3\beta^3} (\sin \beta t - \beta t \cos \beta t) + \cos \beta t + \frac{a_{11} - \beta^2}{2\beta} t \sin \beta t \tag{2-23}$$

In simplified form

$$f_{21}(t) = \frac{1}{2\beta^3}\left[(a_{01} + \beta^2 a_{21}) + (a_{11}\beta^2 - \beta^4)t\right] \sin \beta t + \frac{1}{2\beta^2}\left[2\beta^2 + (a_{21}\beta^2 - a_{01})t\right] \cos \beta t \tag{2-24}$$

To insert the exponential shift, this equation is multiplied by the exponential function $\exp(-\alpha t)$.

The next requirement is a time shift back by five time-constants and a time reversal. The actual time function $\phi_2(t)$ is:

$$\phi_2(t) = \exp(\alpha t - 5T\alpha) f_{21}(5T - t) \tag{2-25}$$

where $T = 1/\alpha$ is the time constant associated with the exponential function.

To simplify calculations, the time reversal was worked out to match the form

$$\phi_2(t) = \exp(\alpha t - 5T\alpha)\left[(Z_1 + Z_2) \sin \beta t + (Z_3 + Z_4) \cos \beta t\right] \tag{2-26}$$

where

$$Z_1 = \frac{-1}{2\beta^3}\left[a_{01} + \beta^2 a_{21} + 5Ta_{11}\beta^2 - 5T\beta^4 - (a_{11}\beta^2 - \beta^4)t\right] \cos 5T\beta \tag{2-27}$$

$$Z_2 = \frac{1}{2\beta^2}\left[2\beta^2 + 5Ta_{21}\beta^2 - 5Ta_{01} - (a_{21}\beta^2 - a_{01})t\right] \sin 5T\beta \tag{2-28}$$

$$Z_3 = -Z_1 \frac{\sin 5T\beta}{\cos 5T\beta} \tag{2-29}$$

$$Z_4 = Z_2 \frac{\cos 5T\beta}{\sin 5T\beta} \tag{2-30}$$

For any given set of constant parameters in a second-order system, the probing signal ϕ_2 can now be easily obtained by introducing specific values in Equations 2-17, 2-18, and 2-19, then into 2-27, 2-28, and 2-29. The resulting probing signal is then given by Equation 2-26.

For the X-Y plotter transfer function in Equation 2-8 the input probing signal is:

$$\phi_2(t) = 3.88 \exp (7.54t - 5) \left[(-3.75 + 10.2t) \sin 11.3t + (20.44 - 37.17t) \cos 11.3t\right] \tag{2-31}$$

The time function for ϕ_1 is:

$$\phi_1(t) = 3.88 \exp (7.54t - 5) (0.757 \sin 11.3t + 0.844 \cos 11.3t) \tag{2-32}$$

The next major step involves the filter coefficients to match these input probing signals. The first function, Equation 2-12, is straightforward and coefficients can be obtained by referring to the computer diagram.

The filter for Equation 2-13 requires splitting up the function into three parts, as follows:

$$\Phi_2(+S) = \Phi_1(+S) \frac{S - \omega_o}{S + \omega_o} \frac{(S - \alpha)^2 + \beta^2}{(S + \alpha)^2 + \beta^2} \tag{2-33}$$

In this form, the coefficients can easily be correlated to the computer diagram (see Figure 2-5).

The next requirement includes the modulation matrix evaluation and the estimator coefficients. The detailed theoretical background for these calculations is discussed in both the Phase A and Phase B reports. For purposes of this report, specific values were introduced in general equations on page 34 of the Phase B report. The results within a scale factor are:

$$H_{d_1} = \begin{bmatrix} -5.51 \times 10^{-5} & 2.815 \times 10^{-4} \\ 0 & -5.51 \times 10^{-5} \end{bmatrix} \tag{2-34}$$

$$H_{d_o} = \begin{bmatrix} -9.18 \times 10^{-6} & 3.67 \times 10^{-5} \\ 0 & -9.18 \times 10^{-5} \end{bmatrix} \quad (2\text{-}35)$$

and the modulation matrix

$$M = 10^{5} \begin{bmatrix} 28.15 & 3.67 \\ -5.51 & -0.918 \end{bmatrix} \quad (2\text{-}36)$$

and the estimator normalized to $d_1 = 15.05$ and $d_o = 184.4$ is:

$$L = 10^{-3} \begin{bmatrix} -1.088 & -4.36 \\ 0.534 & 2.725 \end{bmatrix} \quad (2\text{-}37)$$

The last requirement is the simulation of the actual system transfer function. For this particular practical second-order system, with voltage levels at the low end of the dynamic range of the computer, the simulated transfer function was not sufficient. In light of this limitation, a second X-Y plotter of the same characteristics was used in place of the nominal system. From a practical standpoint, in this instance, it was relatively easy to match the two systems because of the available parameter adjustments and the small physical size which made the extra system readily available.

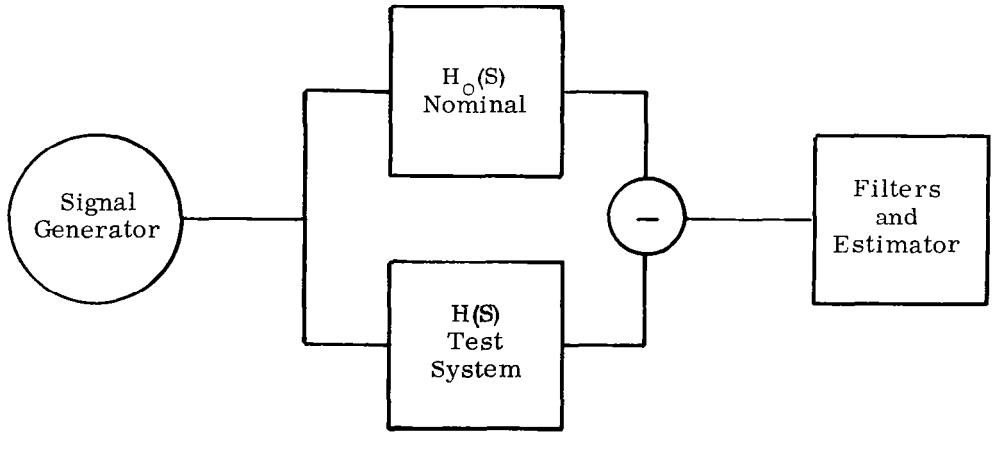

Figure 2-5. General Computer Diagram (for specific circuit details see Figure 3-5, Phase B Report)

SECTION 3

POSITION SYSTEM

INTRODUCTION

Consistent with the objectives of Phase C of single parameter testing, an actual subsystem was chosen for analysis. The subsystem chosen is a position control system. This subsystem is to be analyzed by utilizing the work performed on Phase A and Phase B of the contract.

The purpose of this analysis is obvious. We wish to establish in this phase of the contract that the theory developed in Phase A and Phase B can be applied to a complex transfer function. It is important that the theory be able to measure meaningful parameters and that it measure the least reliable parameters.

The work on this position control system attempts to measure a particular partial derivative of the transfer function. In the examination of the X-Y plotter, the approach was to examine the domain poles and zeros which had the largest effect on the transfer function. While the two examinations are related, the investigation of particular partial derivatives of the transfer function does not make any gross assumption about dominance of any set of poles on zero. It is a more refined approach removing assumptions associated with transfer function approximations.

The positioning system under study has a given transfer function. The transfer function was established by empirical methods on the real system. Therefore, there is one basic assumption associated with the test of the position system. This assumption is related to the degree of accuracy with which the empirical data approximates the actual transfer function. We will assume, in the testing of the positioning system, that the given transfer function is, in fact, the true transfer function.

TRANSFER FUNCTION

The empirical block diagram for this system is shown in Figure 3-1.

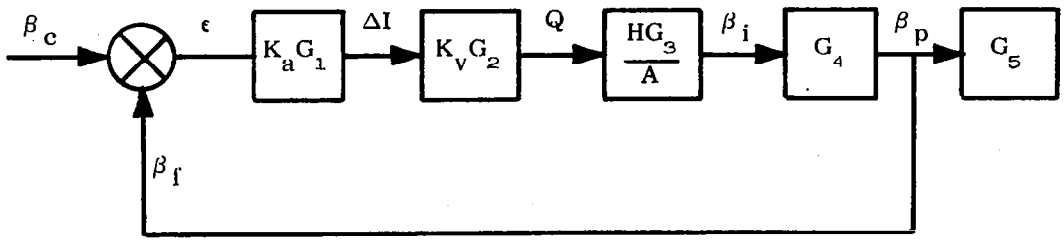

Figure 3-1. System Block Diagram

where

$$K_aG_1 = \frac{9.09}{\left[\frac{S^2}{(300)^2} + \frac{2(0.7)S}{300} + 1\right]} \tag{3-1}$$

$$K_VG_2 = \frac{0.53\left(\frac{S}{18.86} + 1\right)}{\left(\frac{S}{21.45} + 1\right)\left(\frac{S}{377} + 1\right)} \tag{3-2}$$

$$\frac{HG_3}{A} = \frac{2.82}{0.6}\left(\frac{1}{S}\right) \tag{3-3}$$

$$G_4 = \frac{\left[\frac{S^2}{(80.38)^2} + \frac{2(0.05)S}{80.38} + 1\right]}{\left[\frac{S^2}{(70.57)^2} + \frac{2(0.416)S}{70.57} + 1\right]} \tag{3-4}$$

$$G_5 = \frac{1}{\left[\frac{S^2}{(80.38)^2} + \frac{2(0.05)S}{80.38} + 1\right]} \tag{3-5}$$

The open-loop transfer function for this system is:

$$F_oK_o = \frac{K_o\left(\frac{S}{18.86} + 1\right)\left[\frac{S^2}{(80.38)^2} + \frac{2(0.05)S}{80.38} + 1\right]}{S\left(\frac{S}{21.45} + 1\right)\left(\frac{S}{377} + 1\right)\left[\frac{S^2}{(300)^2} + \frac{2(0.7)S}{300} + 1\right]\left[\frac{S^2}{(70.57)^2} + \frac{2(0.416)S}{70.57} + 1\right]} \tag{3-6}$$

where $K_o = 22.64$.

After combining and simplifying the blocks in Figure 3-1, the two blocks in Figure 3-2 are obtained:

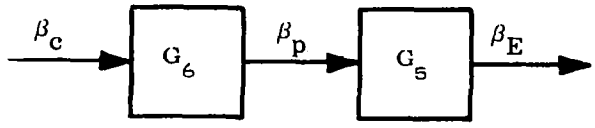

Figure 3-2. Simplified Block Diagram

where

$$G_6 = \frac{\left(\frac{S}{18.86}+1\right)\left[\frac{S^2}{(80.38)^2}+\frac{2(0.05)S}{80.38}+1\right]}{\left(\frac{S}{16.5}+1\right)\left(\frac{S}{64.18}+1\right)\left(\frac{S}{338.9}+1\right)\left[\frac{S^2}{(279.57)^2}+\frac{2(0.745)S}{279.57}+1\right]\left[\frac{S^2}{(54)^2}+\frac{2(0.377)S}{54}+1\right]} \quad (3\text{-}7)$$

$$G_5 = \frac{1}{\left[\frac{S^2}{(80.38)^2}+\frac{2(0.05)S}{80.38}+1\right]} \quad (3\text{-}8)$$

The final results of β_E/β_c are obtained by combining the two blocks in Figure 3-2 and are shown in Figure 3-3.

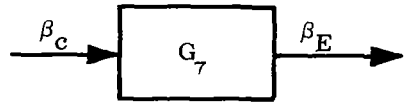

Figure 3-3. Total System Function

where

$$G_7 = \frac{\left(\frac{S}{18.86}+1\right)}{\left(\frac{S}{16.5}+1\right)\left(\frac{S}{64.18}+1\right)\left(\frac{S}{338.9}+1\right)\left[\frac{S^2}{(279.57)^2}+\frac{2(0.745)S}{279.57}+1\right]\left[\frac{S^2}{(54)^2}+\frac{2(0.377)S}{54}+1\right]} \quad (3\text{-}9)$$

The preceding transfer function representing the complete closed-loop system can now be analyzed to determine the dominant poles. The dominance can be expected to be in the following poles:

$$\left(\frac{S}{64.18} + 1\right) \tag{3-10}$$

and

$$\left[\frac{S^2}{(54)^2} + \frac{2(0.377)S}{54} + 1\right] \tag{3-11}$$

The pole at 16.5 is effectively reduced in the transfer function by the zero at 18.86. The other poles have high time-constants and will damp out of the solution in a short period of time.

Evaluating the time response of the system to a unit impulse, the following was obtained:

$$\left.\begin{aligned} f(t) = {} & 3.68\, e^{-16.5t} + 60.8\, e^{-64.14t} - 2.91\, e^{-338.9t} \\ & + 6.06\, e^{-208.3t} \sin(189.6t + 84.35^{\circ}) \\ & + 57.4\, e^{-20.36t} \sin(50.015t - 17.4) \end{aligned}\right\} \tag{3-12}$$

From this time response, it can be observed that the exponential $60.8\, e^{-64.14t}$ is, in fact, the largest term. The complex poles at $\omega = 54$ also contribute to a large part of the time response. The pole at 16.5 does contribute a signal which is approximately four times slower than the pole at 64.14. It, therefore, will also be dominant in the solution after a certain period of time.

It can be concluded that the poles at

$$S = -16.5$$

$$S = -64.14$$

and

$$S = -20.36 \pm j\, 50.015$$

will be dominant parameters of the transfer function. The pole at -16.5 is the result of G_3. The pole at -64.14 is the result of G_2. The poles at $-20.36 \pm j\, 50.015$ are the result of G_5.

G_5 is the mechanical load and is not subject to variations or unreliability. The load will remain relatively the same from system to system.

G_2 is a control valve which controls the amount of fluid flow which positions the load. This valve is one of the more critical parts of the system. Its operation may be expected to vary from system to system, and some degree of reliability can be expected.

G_3 is the actuator system. This portion of the transfer function is expected to be relatively invariant and have a high reliability.

Thus, it can be concluded that of the dominant poles in the transfer function, the pole resulting from the valve is the most critical and should be included in all tests.

The location of the poles in the closed-loop transfer function are related to the open-loop gain. Since the open-loop gain affects the location of the critical poles, it is desirable to measure this gain.

PARTIAL SYSTEMS

A change of the transfer function will result if a particular parameter changes. These changes are described by the Taylor Series Expansion as described in the Phase A report.

$$H(S) = H_o + \frac{\partial H(S)}{\partial \alpha_1} \Delta\alpha_1 + \ldots + \frac{1}{2} \frac{\partial^2 H(S)}{\partial^2 \alpha_1} \Delta\alpha_1^2 \qquad (3\text{-}13)$$

where

H_o = the specified nominal system.

$H_{\alpha_i}(S) = \frac{\partial H(S)}{\partial \alpha_i}$ = first partial derivative of the system with respect to the ith parameter.

α_i = the particular parameter under investigation.

These partial derivative terms are those of primary concern. Considering the closed-loop transfer function of the form

$$H(S) = \frac{(S\tau_1 + 1)}{(S\tau_2 + 1)(S\tau_3 + 1)(S\tau_4 + 1)\left[\frac{S^2}{\omega_5^2} + \frac{2\delta_5 S}{\omega_5} + 1\right]\left[\frac{S^2}{\omega_6^2} + \frac{2\delta_6 S}{\omega_6} + 1\right]} \qquad (3\text{-}14)$$

the partial derivative with respect to a single-order pole is:

$$\frac{\partial H(S)}{\partial \tau_i} = \frac{-S}{(S\tau_i + 1)} H(S) \tag{3-15}$$

and the partial derivative with respect to a complex pole is:

$$\frac{\partial H(S)}{\partial\left(\frac{1}{\omega_j}\right)} = \frac{-\left(\frac{2S^2}{\omega_j} + 2\delta_j S\right) H(S)}{\left(\frac{S^2}{\omega_j^2} + \frac{2\delta_j S}{\omega_j} + 1\right)^2} \tag{3-16}$$

Another partial derivative of major concern is that one taken with respect to the open-loop gain. The closed-loop gain for this particular system is:

$$H(S) = \frac{K_o F_o G_5}{1 + K_o F_o} = \frac{N(S)}{D(S)} \tag{3-17}$$

where

K_o is the open-loop gain.

F_o is the open-loop transfer function.

$$\left.\begin{aligned} \frac{\partial H(S)}{\partial K_o} &= \frac{F_o G_5 - F_o}{(1 + K_o F_o)^2} = \frac{F_o G_5 - F_o}{\left[D(S)\right]^2} \\ &= \frac{H(S)}{K_o\left[D(S)\right]} - \frac{H(S)}{K_o F_o\left[D(S)\right]} \end{aligned}\right\} \tag{3-18}$$

To measure these partial systems it is necessary to develop the orthogonalized signal as reported in the Phase A report. Following the procedures reported in the Phase A report, the following orthogonalized Laplace representation of the signals is obtained:

$$\Phi_1(S) = \sqrt{2\omega_2}\,\frac{1}{S + \omega_2} \tag{3-19}$$

$$\Phi_2(S) = \sqrt{2\omega_3}\,\frac{(S - \omega_2)}{(S + \omega_2)(S + \omega_3)} \tag{3-20}$$

$$\Phi_3(S) = \sqrt{2\omega_4}\ \frac{(S-\omega_2)(S-\omega_3)}{(S+\omega_2)(S+\omega_3)(S+\omega_4)} \tag{3-21}$$

$$\Phi_4(S) = \sqrt{2\omega_5}\ \frac{(S-\omega_2)(S-\omega_3)(S-\omega_4)(S+\omega_5)}{(S+\omega_2)(S+\omega_3)(S+\omega_4)(S^2+2\delta_5\omega_5 S+\omega_5^2)} \tag{3-22}$$

$$\Phi_5(S) = \sqrt{2\omega_6}\ \frac{(S-\omega_2)(S-\omega_3)(S-\omega_4)(S^2-2\delta_5\omega_5 S+\omega_5^2)(S-\omega_6)}{(S+\omega_2)(S+\omega_3)(S+\omega_4)(S^2+2\delta_5\omega_5 S+\omega_5^2)(S^2+2\delta_6\omega_6 S+\omega_6^2)} \tag{3-23}$$

$$\Phi_6'(S) = \sqrt{2\omega_6}\ \frac{(S-\omega_2)(S-\omega_3)(S-\omega_4)(S^2-2\delta_5\omega_5 S+\omega_5^2)(S^2-2\delta_6\omega_6 S+\omega_6^2)(S+\omega_6)}{(S+\omega_2)(S+\omega_3)(S+\omega_4)(S^2+2\delta_5\omega_5 S+\omega_5^2)(S^2+2\delta_6\omega_6 S+\omega_6^2)} \tag{3-24}$$

$$\Phi_6''(S) = \sqrt{2\omega_2}\ \frac{(S-\omega_2)(S-\omega_3)(S-\omega_4)(S^2-2\delta_5\omega_5 S+\omega_5^2)(S^2-2\delta_6\omega_6 S+\omega_6^2)}{(S+\omega_2)^2(S+\omega_3)(S+\omega_4)(S^2+2\delta_5\omega_5 S+\omega_5^2)(S^2+2\delta_6\omega_6 S+\omega_6^2)} \tag{3-25}$$

$$\Phi_7(S) = \sqrt{2\omega_3}\ \frac{(S-\omega_2)^2(S-\omega_3)(S-\omega_4)(S^2-2\delta_5\omega_5 S+\omega_5^2)(S^2-2\delta_6\omega_6 S+\omega_6^2)}{(S+\omega_2)^2(S+\omega_3)^2(S+\omega_4)(S^2+2\delta_5\omega_5 S+\omega_5^2)(S^2+2\delta_6\omega_6 S+\omega_6^2)} \tag{3-26}$$

$$\Phi_8(S) = \sqrt{2\omega_4}\ \frac{(S-\omega_2)^2(S-\omega_3)^2(S-\omega_4)(S^2-2\delta_5\omega_5 S+\omega_5^2)(S^2-2\delta_6\omega_6 S+\omega_6^2)}{(S+\omega_2)^2(S+\omega_3)^2(S+\omega_4)^2(S^2+2\delta_5\omega_5 S+\omega_5^2)(S^2+2\delta_6\omega_6 S+\omega_6^2)} \tag{3-27}$$

$$\Phi_9(S) = \sqrt{2\omega_5}\ \frac{(S-\omega_2)^2(S-\omega_3)^2(S-\omega_4)^2(S-\omega_5)(S^2-2\delta_5\omega_5 S+\omega_5^2)(S^2-2\delta_6\omega_6 S+\omega_6^2)}{(S+\omega_2)^2(S+\omega_3)^2(S+\omega_4)^2(S^2+2\delta_5\omega_5 S+\omega_5^2)^2(S^2+2\delta_6\omega_6 S+\omega_6^2)} \tag{3-28}$$

$$\Phi_{10}(S) = \sqrt{2\omega_5}\ \frac{(S+\omega_5)(S-\omega_2)^2(S-\omega_3)^2(S-\omega_4)^2(S^2-2\delta_5\omega_5 S+\omega_5^2)^2(S^2-2\delta_6\omega_6 S+\omega_6^2)}{(S+\omega_2)^2(S+\omega_3)^2(S+\omega_4)^2(S^2+2\delta_5\omega_5 S+\omega_5^2)^2(S^2+2\delta_6\omega_6 S+\omega_6^2)^2} \tag{3-29}$$

Some linear combination of $\Phi_{10}(S)$ with the other signals will measure the open-loop gain.

Some linear combination of $\Phi_6''(S)$ with the other $\Phi_n(S)$, where $n < 6$, will be required to measure the effect of a single-order pole.

Some linear combination of $\Phi_6'(S)$ with the other $\Phi_n(S)$, where $n < 6$, will be required to measure the effect of a complex single-order set of poles.

Therefore, it is necessary to find the optimum probing signal which will be matched to the partial system to be measured, and reduce the coupling between measurements of the partial system parameters.

The next section will introduce the procedure and the approach which will be taken to arrive at the probing signal.

TESTING FUNCTIONS

To test the important parameters of the positioning system, the procedures reported in Phase A will be followed. However, analog simulation will be used to obtain signals instead of analog simulation of a signal generator.

The reason for adopting analog simulation is that the orthogonal signals have become complex and high ordered. In order to take the inverse Laplace transform and obtain the time response for each signal would be time-consuming. Therefore, the Laplace representation of the signals will be simulated and the resulting filters will be impulsed. The procedure is illustrated in Figure 3-4. The impulse response will then be the respective time functions. By using analog simulation the resulting time functions will be reversed in time and used as stimuli in testing the actual simulated transfer function $H_{\alpha_i}(S)$.

The resulting orthogonalized signals when impressed upon the system to be measured [the partial system $H_{\alpha_i}(S)$] will then result in a partial value at the output of the measuring filters at time $t = 0$. This procedure is described in more detail in the Phase A report, but in general the result can be illustrated as shown in Figure 3-5.

These measurements at the output of the filters determine the h_{jk} of the matrix representation given in Equation 3-29 of the Phase A report. This matrix represents the result of the input signal acting on the $H_{\alpha_i}(S)$ partial system and the measuring filter $\Phi_j(S)$.

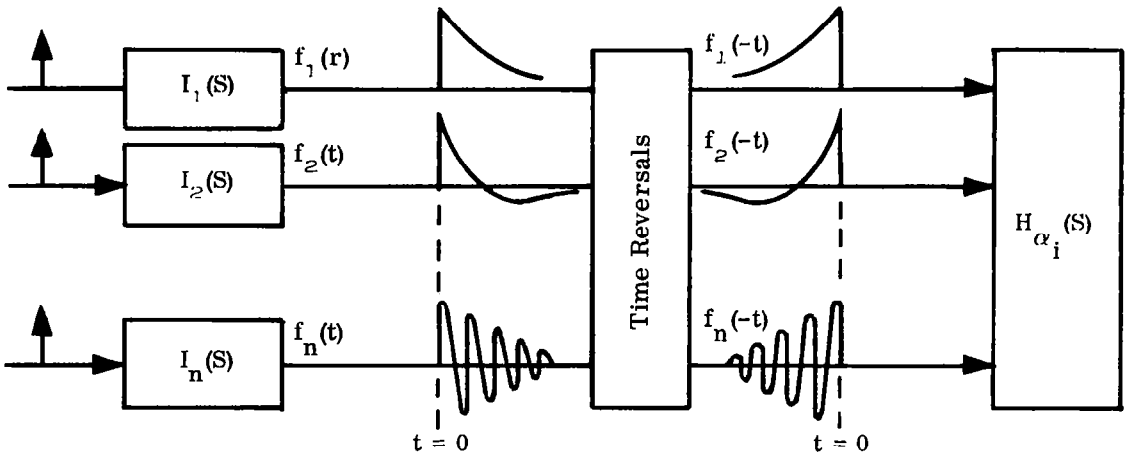

Figure 3-4. Orthogonal Signal Generator

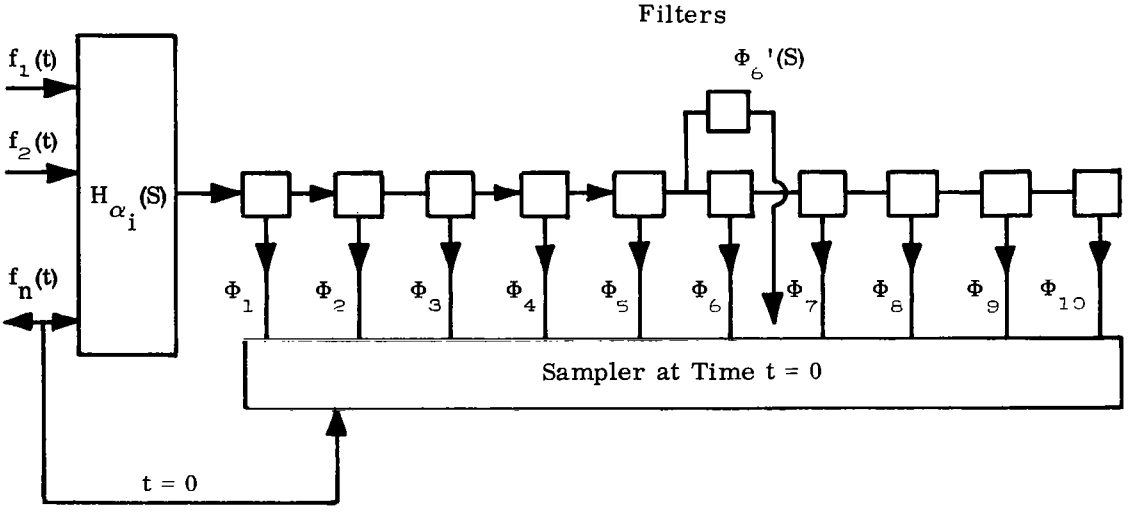

Figure 3-5. Filter and Estimator

Once these matrices are determined for the sensitive partial systems, they will be combined as in the Phase A report to obtain a modulation matrix. This matrix will have to be adjusted by selecting the proper magnitudes of the testing signals to reduce the interference in measuring the particular parameters.

At this point the approach becomes limited. The selection of the proper modulation matrix is a great problem.

One approach under consideration to solve this problem is research to obtain a set of algorithms to maximize the determinant of the modulation matrix. If these algorithms can be developed, a solution will be available by programming a digital computer to obtain both the maximum value of the determinant and the proper values of the magnitude of the signals which maximize the determinant. Other approaches are being considered but have not been sufficiently developed to be of any benefit.

TESTING PROCEDURE

Once the proper input signal has been obtained, analog simulation will be used to evaluate the resulting testing. The program developed to obtain orthogonal signals as the generating source of signals for testing the total transfer function will be used. This should reduce the programming and running time necessary to obtain the measurements.

REFERENCES

1. Truxal, J.G., Control System Synthesis, McGraw-Hill Book Company, Inc., New York, N.Y., 1955.

2. D'Azzo, J., and Houpis, C., Control System Analysis and Synthesis, McGraw-Hill Book Company, Inc., New York, N.Y., 1960.

3. "Servo Motors, Synchros, AC Tachometer Generators," Technical Information, Kearfott Company, Inc.

4. Single Parameter Testing Phase A Completion Report, 65 SIMAR 59/2.

5. Single Parameter Testing Phase B Completion Report, 65 SIMAR 68/7.